

Amino acid residues conferring herbicide resistance in tobacco acetohydroxy acid synthase

Sun-Mi JUNG*, Dung Tien LE*, Sung-Sook YOON*, Moon-Young YOON†, Young Tae KIM‡ and Jung-Do CHOI*¹

*School of Life Sciences and Biotechnology Research Institute, Chungbuk National University, Cheongju 361-763, Korea, †Department of Chemistry, Hanyang University, Seoul 133-791, Korea, and ‡Department of Microbiology, Pukyong National University, Busan 608-737, Korea

The enzyme AHAS (acetohydroxy acid synthase), which is involved in the biosynthesis of valine, leucine and isoleucine, is the target of several classes of herbicides. A model of tobacco AHAS was generated based on the X-ray structure of yeast AHAS. Well conserved residues at the herbicide-binding site were identified, and the roles of three of these residues (Phe-205, Val-570 and Phe-577) were determined by site-directed mutagenesis. The Phe-205 mutants F205A, F205H, F205W and F205Y showed markedly decreased levels of catalytic efficiency, and cross-resistance to two or three classes of herbicides, i.e. Londax (a sulphonylurea herbicide), Cadre (an imidazolinone herbicide) and TP (a triazolopyrimidine derivative). None of the mutations caused significant changes in the secondary or tertiary structure of the enzyme. Four mutants of Phe-577, i.e. F577D, F577E, F577K and F577R, showed unaltered V_{\max} values, but substantially decreased catalytic efficiency. However, these mutants were highly resistant to two or three of the tested herbicides. The three mutants F577D, F577E and F577R had a similar secondary structure to that of wild-type AHAS. Conservative mutations

of Phe-577, i.e. F577W and F577Y, did not affect the kinetic properties of the enzyme or its inhibition by herbicides. The mutation Val-570 to Asn abolished the binding affinity of the enzyme for FAD as well as its activity, and also caused a change in the tertiary structure of AHAS. However, the mutant V570Q was active, but resistant to two classes of herbicides, i.e. Londax and TP. The conservative mutant V570I was substantially reduced in catalytic efficiency and moderately resistant to the three herbicides. The results of this study suggest that residues Phe-205, Val-570 and Phe-577 in tobacco AHAS are located at or near the binding site that is common for the three classes of herbicides. In addition, Phe-205 and Val-570 are probably located at the herbicide-binding site that may overlap partially with the active site. Selected mutants of Phe-577 are expected to be utilized to construct herbicide-resistant transgenic plants.

Key words: acetohydroxy acid synthase, conserved amino acids, herbicide, homology modelling, site-directed mutagenesis, tobacco.

INTRODUCTION

The first enzymic step common to the biosynthesis of branched-chain amino acids is catalysed by AHAS [acetohydroxy acid synthase; EC 2.2.1.6 (formerly EC 4.1.3.18; also known as aceto-lactate synthase)]. The enzyme catalyses two parallel reactions: the condensation of two molecules of pyruvate to give rise to 2-acetolactate in the first step of the valine and leucine synthetic pathway, and the condensation of pyruvate and 2-oxobutyrate to yield 2-aceto-2-hydroxybutyrate in the second step of isoleucine biosynthesis [1,2]. AHAS is a key regulatory enzyme for levels of branched-chain amino acids in both prokaryotes and eukaryotes. Control involves feedback inhibition of the enzyme activity by end-product amino acids, or repression of the biosynthesis of the enzyme [1]. AHAS requires three cofactors for its catalytic activity: TPP (thiamine pyrophosphate), FAD and bivalent metal ions (Mg^{2+} or Mn^{2+}) [3].

AHAS activity is found in bacteria, yeast and plants. Three bacterial AHAS isoenzymes have been purified and studied extensively with respect to their genetic regulation, kinetic properties, feedback regulation and sensitivity to herbicidal inhibitors [4–8]. However, the structure and enzymic properties of AHAS from eukaryotes have not been well characterized, since the purification of AHAS from eukaryotes is difficult due to its extreme instability and very low abundance [1]. A number of AHAS genes from plants, including *Arabidopsis thaliana* [9], *Brassica napus*

[10], *Gossypium hirsutum* [11], *Nicotina tabacum* (tobacco) [9], *Zea mays* [12] and *Xanthium* sp. [13], have been cloned and characterized. AHAS genes from *A. thaliana* [14] and tobacco [15] have been functionally expressed in *Escherichia coli*, and each of the enzymes has been purified.

AHAS has attracted much recent interest since it was found to be the target of several classes of modern and potent herbicides, including the sulphonylureas [16,17], the imidazolinones [18] and the triazolopyrimidines [19,20]. The AHAS-inhibiting herbicides do not compete with the substrates, the cofactors or the feedback inhibitors, and thus the inhibition mechanism is complex [1]. However, the molecular basis for most of the characterized herbicide resistance is simply due to a change in a single amino acid residue from the wild-type AHAS sequence. The various herbicide-resistant mutants from plants have been obtained by spontaneous mutation under field conditions and by site-directed mutation based on structural models and homology searches of AHAS (summarized in [1]). The most common natural mutations in plants involve the residues Ala-121, Pro-187, Pro-196, Trp-573 and Ser-652 (*N. tabacum* numbering) [1]. Site-directed mutagenesis studies on tobacco AHAS in our laboratory revealed that Trp-573 [21], Ala-121 and Ser-652 [22], His-351 [23], Lys-255 [24], and Met-350 and Met-569 [25] are probably located at the herbicide-binding site. More recently, crystallization and preliminary X-ray diffraction analysis of the catalytic subunit of yeast AHAS have been reported [26,27].

Abbreviations used: AHAS, acetohydroxy acid synthase; mAHAS, mutant AHAS; wAHAS, wild-type AHAS; LB, Luria-Bertani; RMS, root mean square; RMSD, root mean square distance; TPP, thiamine pyrophosphate.

¹ To whom correspondence should be addressed (email jdchoi@cbucc.chungbuk.ac.kr).

Alignment of the tobacco and yeast AHAS sequences revealed 41% and 63% sequence identity and similarity respectively. Thus we carried out homology modelling of the catalytic subunit of tobacco AHAS based on the X-ray structure of yeast AHAS using Deep View, and remote automatic modelling with Swiss-Model server [28,29]. The three residues Phe-205, Val-570 and Phe-577 were highly conserved among 39 AHAS sequences of 33 species, and were located at the herbicide-binding site in the model. Accordingly, we carried out site-directed mutagenesis of these three residues and analysed the effects of the mutations on the enzymic properties, the inhibition by herbicides and the structure of the enzyme. In turn, the site-directed mutagenesis data may indicate whether our constructed model is reliable.

MATERIALS AND METHODS

Materials

LB (Luria–Bertani) broth–Miller and LB agar–Miller were purchased from Difco Laboratories (Detroit, MI, U.S.A.). Restriction enzymes were purchased from Roche Co. (Mannheim, Germany). GSH, Sephadex G-25, TPP, FAD, α -naphthol and creatine were obtained from Sigma Chemical Co. (St. Louis, MO, U.S.A.). Thrombin protease and epoxy-activated Sepharose 6B were obtained from Pharmacia Biotech (Uppsala, Sweden). *E. coli* XL1-Blue cells containing the expression vector pGEX-AHAS were provided by Dr Soo-Ik Chang (Chungbuk National University, Cheongju, Korea). Oligonucleotides were obtained from Genotech (Taejon, Korea). Londax (a sulphonylurea herbicide) and Cadre (an imidazolinone herbicide) were provided by Dr Dae-Whang Kim (Korea Research Institute of Chemical Technology, Taejon, Korea). TP, a triazolopyrimidine derivative, was obtained from Dr. Sung-Keon Namgoong (Seoul Women's University, Seoul, Korea).

Homology modelling of the tobacco AHAS catalytic subunit

AHAS sequences from tobacco and yeast were aligned using the BioEdit program [30]. A stretch of 92 N-terminal amino acid residues of tobacco AHAS (corresponding to the transit peptide) were removed, and the resulting sequence was fitted on the X-ray of structure of yeast AHAS using Deep View. The resulting alignment was examined manually and then submitted for automatic modelling to the Swiss-Model server [28,29]. Using this approach, a model of a single catalytic subunit of tobacco AHAS was successfully obtained. The modelling job was then carried out using the oligomer modelling approach as described on the Swiss-Model website (<http://swissmodel.expasy.org>). Homodimer models of tobacco AHAS were obtained. A single round of energy minimization was done with the GROMOS96 implemented on Deep View. Structural illustrations were created from co-ordinate files with Deep View [29] and the Molw PDB Viewer 4.0 with Showcase (<http://www.molimage.com>).

Multiple sequence alignment of AHAS genes

We aligned the sequences of 39 AHAS enzymes from 33 species using the Clustal W program [31], which was integrated into the BioEdit software [30] provided by North Carolina State University (Figure 1). The data set consisted of AHAS sequences from following species (GenBank accession numbers are given in parentheses): *Amaranthus powellii* (AAK50821), *Amaranthus retroflexus* (AAK50820), *Amaranthus* sp. (AAB67839), *Arabidopsis thaliana* (P17597), *Brassica napus* (P27818, P14874 and P27819), *Bassia scoparia* (AAC69629), *Cyanidium calda-*

	F205	V570	F577
<i>A. powellii</i>	RIVKEAFFLA	LGMVQVQME	DR FFKAN-
<i>A. retroflexus</i>	RIVKEAFFLA	LGMVQVQME	DR FFKAN-
<i>A. spp.</i>	RIVKEAFFLA	LGMVQVQLE	DR FFKAN-
<i>A. thaliana</i>	RIIEEAFFLA	LGMVMQVME	DR FFKAN-
<i>B. napus ALS I</i>	RIVQEAFFLA	LGMVMQVME	DR FFKAN-
<i>B. napus ALS II</i>	RIVREAFFLA	LGMVLQVME	DH FFAAN-
<i>B. napus ALS III</i>	RIVQEAFFLA	LGMVMQVME	DR FFKAN-
<i>B. scoparia *</i>	RIVKEAFFLA	LGMVQVQLE	DR FFKAN-
<i>C. caldarium</i>	TIVSEAFYIS	IGMVRQVQQA	FYDQR-
<i>Guillardia theta</i>	KIVAESFFIA	IGMVRQVQQA	FYGER-
<i>N. tabacum SuRA</i>	RVVREAFFLA	LGMVQVQME	DR FFKAN-
<i>N. tabacum SuRB</i>	RVVREAFFLA	LGMVQVQME	DR FFKAN-
<i>P. purpurea</i>	RIVAEAFYIC	IGMVRQVQQA	FYGER-
<i>R. raphanistrum</i>	RIVQEAFFLA	LGMVMQVME	DR FFKAN-
<i>S. platensis</i>	RIVVEAFHLA	LGMVRQVQQA	HM FYNDR-
<i>S. ptychanthum</i>	RIVREAFFLA	LGMVQVQME	DR FFKAN-
<i>Volvox carteri</i>	RVIKEAFYLA	LGMVQVQME	DR FFKAN-
<i>B. subtilis ILVB</i>	RIIKEAFHIA	LGMVRQVQEI	FYEER-
<i>B. subtilis ILVX</i>	EAVTNAFRIA	YDMVAFQQLK	KYNRT-
<i>A. pisum</i>	IVFKKAFVLA	LGMVKQVQDM	IYSGR-
<i>S. graminum</i>	IIFKKAFVLA	LGMVKQVQDM	IYSGR-
<i>S. chinensis</i>	ITFKKAFVLA	LGMVKQVQDI	IYSGR-
<i>C. acetobutylicum</i>	EIVRKAFKTA	YGLIKWKQEE	RYGES-
<i>C. glutamicum</i>	QALAEAFHLA	LGMVRQVQTL	FYEGR-
<i>E. coli ALS I</i>	QVMSDAFRIA	LGLVHQVQSL	FYEQQV-
<i>E. coli ALS II</i>	RIMAEAFDVA	LGMVRQVQQL	FFQER-
<i>E. coli ALS III</i>	QVLKKAFLA	LGMVKQVQDM	IYSGR-
<i>H. influenzae</i>	STLKKAFYIA	LGMVKQVQDL	IYSGR-
<i>K. pneumoniae</i>	EVVSNAFRAA	YNMVAIQEK	KYQRL-
<i>L. lactis sub. lactis</i>	RIVTEAYYLA	LGMVRQVQES	FYEER-
<i>M. grisea</i>	RRINEAFEIA	IGMVTQVQNL	FYEDR-
<i>M. jannaschii</i>	ETFRAAFEIA	LGMVYQVQNL	YYGQR-
<i>M. avium</i>	AVLAEAFHIA	LGMVRQVQTL	FYEER-
<i>M. leprae</i>	RVLAEAFHIA	LGMVRQVQAL	FYQER-
<i>M. tuberculosis</i>	RVLAEAFHIA	LGMVRQVQSL	FYAER-
<i>R. terrigena</i>	EVVSNAFRAA	YNMVAIQEK	KYQRL-
<i>S. cerevisiae</i>	LRINEAFEIA	IGMVTQVQSL	FYEHR-
<i>S. typhimurium</i>	LVLKKAFLA	LGMVKQVQDM	IYSGR-
<i>S. pombe</i>	RRIDEAFEIA	IGMVTQVQNL	FYEKR-

Figure 1 Multiple sequence alignment of 39 AHAS sequences from plants and micro-organisms showing the degree of conservation of Phe-205, Val-570 and Phe-577

Residue numbering is that of tobacco AHAS. Organism names are listed in full in the text.

rium (O19929), *Guillardia theta* (O78518), *Nicotina tabacum* (CAA30484 and CAA30485), *Porphyra purpurea* (P31594), *Raphanus raphanistrum* (CAC86696), *Spirulina platensis* (P27868), *Solanum ptychanthum* (AAG40281), *Volvox carteri* (AAC04854), *Bacillus subtilis* (P37251 and Q04789), *Acyrtosiphon pisum* (P57321), *Schizaphis graminum* (O85293), *Schlechtendalia chinensis* (Q9RQ65), *Clostridium acetobutylicum* (AAC06204), *Corynebacterium glutamicum* (P42463), *Escherichia coli* (P08142, P00892 and P00893), *Haemophilus influenzae* (P45261), *Klebsiella pneumoniae* (P27696), *Lactococcus lactis sub. lactis* (Q02137), *Magnaporthe grisea* (AAB81248), *Methanocaldococcus jannaschii* (Q57725), *Mycobacterium avium* (Q59498), *Mycobacterium leprae* (O33112),

Mycobacterium tuberculosis (O53250), *Raoultella terrigena* (Q04524), *Saccharomyces cerevisiae* (P07342), *Salmonella typhimurium* (P40811) and *Schizosaccharomyces pombe* (P36620).

Site-directed mutagenesis

Site-directed mutagenesis of tobacco AHAS was performed directly on the plasmid derived from pGEX-2T containing tobacco AHAS cDNA, using the PCR megaprimer method [32]. All DNA manipulations were carried out using the technique reported previously [33]. PCR was also performed as described previously [34]. The first PCR was carried out with oligonucleotide primer NKB2 and the relevant mutagenic fragment as internal primers. Primers were as follows (underlined bases are changed; the bases shown in bold are *Bam*HI restriction sites): NKB1, 5'-CAT CAC **CGG** ATC CAT GTC CAC TAC CCA A-3'; NKB2, 5'-CCC GGG **GAT** CCT CAA AGT CAA TA-3'; F205A, 5'-TGA TGC TGC **CCA** GGA AAC TCC-3'; F205H, 5'-TGA TGC TCA **CCA** GGA AAC TCC-3'; F205W, 5'-TGA TGC **TTG** GCA GGA AAC TCC-3'; F205Y, 5'-TGA TGC **TTA** CCA GGA AAC TCC-3'; F577D, 5'-ATC GGG **ACT** ATA AGG CTA AC-3'; F577E, 5'-ATC GGG **AAT** ATA AGG CTA AC-3'; F577K, 5'-ATC GGA **AAT** ATA AGG CTA AC-3'; F577R, 5'-ATC GGA **GGT** ATA AGG CTA ACA G-3'; V570I, 5'-GGA ATG **ATC** GTT CAA TGG GAG G-3'; V570N, 5'-GGA ATG **AA**C GTT CAA TGG GAG G-3'; V570Q, 5'-GGA ATG **CAG** GTT CAA TGG GAG G-3'.

Each reaction mixture contained 100 ng of template DNA, 10 pmol of mutagenic primer, 10 pmol of universal primer NKB2 and 2.5 mM of each dNTP in 100 mM KCl, 200 mM Tris (pH 8.8), 100 mM (NH₄)₂SO₄, 20 mM MgSO₄, 1% Triton X-100 and 1 mg/ml acetylated BSA in 50 μ l. Each reaction was performed for 30 cycles of the following program: 94 °C for 50 s, 58–60 °C for 1 min and 72 °C for 1 min. The resulting DNA was subjected to a second PCR with the universal primer NKB1. The reaction for the second PCR was performed for 30 cycles of the following program: 94 °C for 55 s, 56 °C for 1 min and 72 °C for 90 s. The PCR products were double-digested with *Nco*I and *Bgl*II and cloned into the expression vector, which was prepared from *Nco*I/*Bgl*II-excised pGEX-wAHAS (where wAHAS is wild-type AHAS). The resulting pGEX-mAHAS (where mAHAS is mutant AHAS) was used to transform *E. coli* XL1-Blue cells using standard CaCl₂ transformation instructions [33].

DNA sequence analysis

Each transformant was sequenced to ensure the presence of the correct base mutation in the mutant AHAS gene. DNA sequencing was carried out with primer SSP1 (5'-GGA TCC ATG TCCACT ACC CAA-3') or SSP3 (5'-GGC GTT ACA GGG TTT GAA TTC G-3') by Macrogen Co. (Seoul, Korea).

Expression and purification of tobacco wAHAS and mAHAS

Bacterial strains of *E. coli* BL21-DE3 cells containing the expression vector pGEX-AHAS were grown at 37 °C in LB medium containing 50 μ g/ml ampicillin to a *D*₆₀₀ of 0.7–0.8. Expression of pGEX-AHAS was induced by adding 0.3 mM isopropyl β -D-thiogalactoside. Cells were grown for an additional 3–4 h at 30 °C, and then harvested by centrifugation at 5000 *g* for 30 min. Purification of wAHAS and mAHAS was carried out as described previously by Chang et al. [15]. The isolated protein was identified by SDS/PAGE analysis [35], and the protein concentration was determined by the method of Bradford [36].

Enzyme assay and determination of kinetic parameters

Enzyme activities of purified wAHAS and mAHAS were measured according to the method of Westerfeld [37] with a modification as reported previously [38]. The reaction mixture contained 20 mM potassium phosphate buffer (pH 7.5), 0.4 mM TPP, 4 mM MgCl₂, 8 μ M FAD, 40 mM pyruvate and the enzyme in the absence or presence of various concentrations of inhibitors.

The values of V_{\max} and K_m for the substrate were determined by fitting the data into eqn (1), while the values of K_c were obtained by fitting the data into eqn (2), by the non-linear least-squares and Simplex methods for error minimization [39]:

$$v = V_{\max}/(1 + K_m/[S]) \quad (1)$$

$$v = V_0 + V_{\max}/(1 + K_c/[C]) \quad (2)$$

In these equations, v is the reaction velocity, V_{\max} is the maximum velocity, V_0 is the activity without adding cofactors (due to the trace of cofactors present in the enzyme solution), K_m is the Michaelis–Menten constant, K_c is the activation constant, $[S]$ is the substrate concentration and $[C]$ is the concentration of added cofactors. K_i^{app} values were determined by fitting the data into eqn (3):

$$v_i = v_0/(1 + [I]/K_i^{\text{app}}) \quad (3)$$

In this equation, v_i and v_0 represent the rate in the presence and absence of the inhibitor respectively, and $[I]$ is the inhibitor concentration. K_i^{app} is the apparent K_i , i.e. the concentration of the inhibitor giving 50% inhibition under standard assay conditions (also known as the IC₅₀).

Spectroscopic measurements

Absorption spectra were recorded on a Beckman DU-650 spectrophotometer. The protein solution was dispensed in a 1 ml black-walled quartz cuvette, and the spectrum of each sample was scanned over the range 250–550 nm. Fluorescence emission spectra were recorded with a Hitachi F-3000 fluorescence spectrophotometer. The fluorescence spectra of FAD bound to wAHAS and mAHAS were scanned over the range 450–700 nm by exciting at 370 nm. The CD spectra were recorded over the range 190–250 nm or 240–320 nm on a Jasco J-710 spectropolarimeter set at 20–50 mdeg sensitivity, 0.2 nm resolution, 3 units accumulation, 1 s response, and a scanning speed of 20 nm/min. A protein solution of 0.25–0.50 mg/ml was assayed in a 1 mm path-length cylindrical quartz cell or a 20 mm path-length cylindrical quartz cell.

RESULTS

Multiple sequence alignment and homology modelling

A total of 39 AHAS sequences from 33 species were aligned using Clustal W [31] implemented within BioEdit software [30]. It was observed that the three residues Phe-205, Val-570 and Phe-577 (tobacco AHAS numbering) were highly conserved among 39 AHAS sequences (Figure 1). Pairwise alignment of tobacco AHAS and yeast AHAS for homology modelling revealed 41% and 63% sequence identity and similarity respectively. Thus a homology model of tobacco AHAS was constructed based on the X-ray structure of yeast AHAS using Deep View and the Swiss-Model server [28,29]. The homology model was shown to be

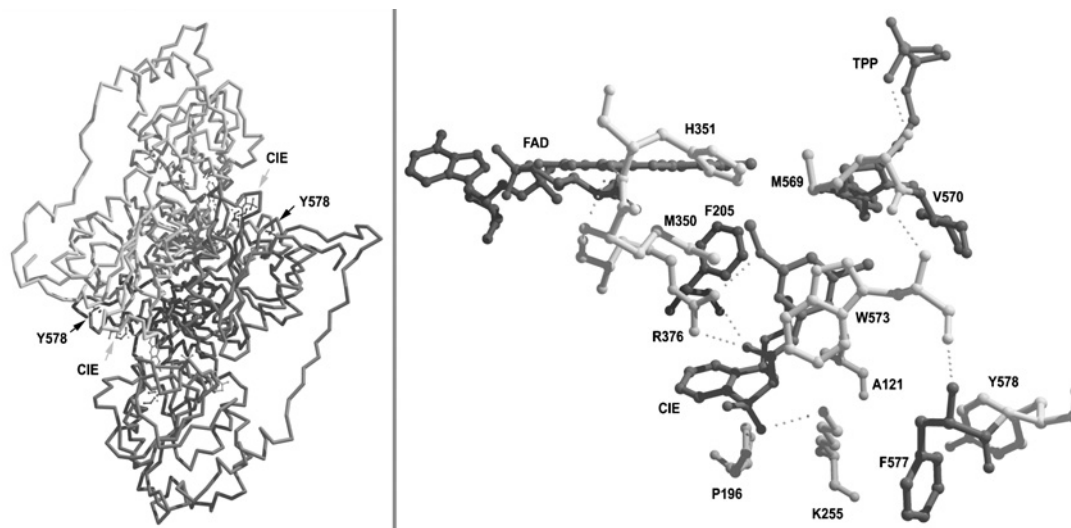


Figure 2 Molecular model of tobacco AHAS

The model was constructed based on a yeast AHAS template using Deep View and the Swiss-Model server (see the Materials and methods section for details). Left, dimer model of tobacco AHAS; right, herbicide-binding site. CIE (chlorimuron ethyl) is a sulphonylurea. Dotted lines connect two atoms within hydrogen-bonding distance. The figure was generated with Molw PDB viewer 4.0 and Showcase from the model co-ordinate.

reliable by its Ramachandran plot (results not shown), its RMS (root mean square) Z -score (results not shown) and a pairwise RMSD (root mean square distance) value of 0.86 Å when the tobacco AHAS model was superimposed on the yeast AHAS structure (results not shown).

Prediction of amino acid residues at the herbicide-binding site

Based on the homology model, seven residues of monomer A and 11 residues of monomer B are located within 5 Å of the putative binding site for a sulphonylurea, chlorimuron ethyl (Figure 2; other six residues not shown). Of these, His-351 [23], Met-350, Met-569 [25] and Trp-573 [21] of monomer A, and Ala-121 [22], Pro-196 [1] and Lys-255 [24] of monomer B, have been reported to be involved in the binding of herbicides, as indicated by site-directed mutagenesis experiments. In the present study, the three residues Phe-205, Val-570 and Phe-577, which are well conserved and predicted to be at the herbicide-binding site, were subjected to site-directed mutagenesis.

Expression and purification of tobacco AHAS

All mutants were expressed as soluble proteins and purified to homogeneity by two steps of affinity chromatography, which employed a GSH-coupled Sepharose 6B column (see the Materials and methods section for details). The expression profiles of the mutants were similar to that of the wild type, and the SDS/PAGE data showed that all mutants had the same molecular mass (65 kDa) as the wild-type enzyme (results not shown).

Phe-205 mutants of AHAS

The mutants and wild-type enzyme were characterized with respect to their kinetic properties and K_i^{app} values for three herbicides: Londax (a sulphonylurea), Cadre (an imidazolinone) and TP (a triazolopyrimidine) (Table 1). The structures of the three herbicides are shown in Figure 3. The substrate and cofactor saturation curves for wAHAS and the mutants F205A, F205H,

F205W and F205Y were hyperbolic (results not shown), as reported previously for wAHAS [13].

Table 1 shows the values of V_{max} , K_m and V_{max}/K_m for the substrate, K_c for the cofactors, and K_i^{app} for inhibition by herbicides. Mutation of Phe-205 resulted in greatly decreased enzymic activity. The V_{max} values of F205A, F205H, F205W and F205Y were 0.015, 0.43, 0.06 and 0.56 unit/mg respectively, values that are approx. 4–100-fold lower than that of wAHAS. The K_m values for pyruvate and K_c values for FAD of the Phe-205 mutants were not significantly different from those of wAHAS. However, the K_c for TPP of F205W was greatly decreased, while the values of F205A, F205H and F205Y were similar to that of wAHAS (Table 1).

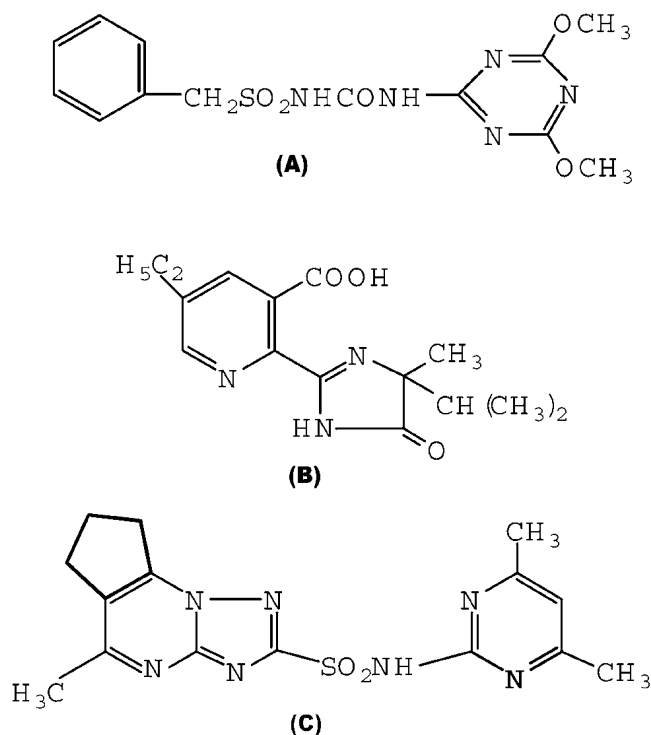
The sensitivities of the Phe-205 mutants to herbicides were determined for three classes of herbicides. These herbicides, i.e. Londax, Cadre and TP, are very potent inhibitors of wAHAS, with K_i^{app} values of 26 nM, 2 μM and 16 μM respectively (Table 1). F205H mutant showed strong resistance to all three herbicides. The F205A mutant was cross-resistant to Londax and Cadre, while F205W and F205Y were strongly cross-resistant to Londax/Cadre and Londax/TP respectively (Table 1 and Figures 4A–4C).

The secondary structure of a protein can be determined by its CD spectrum in the far-UV region (190–250 nm). At these wavelengths, the chromophore is the peptide bond, and the signal arises when it is located in a regular, folded environment [40]. When the CD spectra of the Phe-205 mutants in the far-UV region were compared with that of wAHAS, as shown in Figure 5(A) (and results not shown), the spectra of the Phe-205 mutants overlapped almost completely with that of wAHAS, indicating that no substantial change had occurred in the secondary structure caused by the mutations. The CD spectrum of a protein in the near-UV spectral region (250–350 nm) is sensitive to certain aspects of tertiary structure [40]. At these wavelengths, the chromophores are aromatic amino acids and disulphide bonds, and the CD signals are sensitive to the overall tertiary structure of the protein [40]. Figure 5(B) (and results not shown) shows that the CD spectra of the Phe-205 mutants in the near-UV region overlapped almost completely with that of wAHAS. Thus the tertiary structure

Table 1 Kinetic properties and K_i^{app} values of wAHAS and mutants

For each enzyme, the values shown are the best-fit estimations of parameters obtained from regression analysis. N.D., not detectable within the concentration range 0–128 μM . K_m and V_{max} values are for the substrate pyruvate.

Enzyme	K_m (mM)	V_{max} (units/mg)	V_{max}/K_m	K_c		K_i^{app} for inhibitors		
				FAD (μM)	TPP (mM)	Londax (nM)	Cadre (μM)	TP (μM)
wAHAS	7.33 ± 2.35	1.55 ± 0.09	211×10^{-3}	7.18	0.09	26	2	16
F205A	3.68 ± 1.05	0.015 ± 0.0001	4.1×10^{-3}	4.64	0.41	N.D.	12	14
F205H	53.86 ± 25.34	0.43 ± 0.05	8×10^{-3}	8.52	0.22	N.D.	N.D.	N.D.
F205W	40.99 ± 27.9	0.06 ± 0.01	1.5×10^{-3}	17.95	0.002	N.D.	N.D.	6
F205Y	30.41 ± 12.16	0.56 ± 0.05	18×10^{-3}	11.71	0.8	N.D.	12	N.D.
V570I	58.58 ± 14.02	0.41 ± 0.02	7×10^{-3}	4.2	0.62	19	16	33
V570N	No activity	–	–	–	–	–	–	–
V570Q	129.22 ± 26.51	0.38 ± 0.02	2.9×10^{-3}	48.1	1.17	N.D.	19	N.D.
F577D	24.88 ± 12.88	0.79 ± 0.09	31.8×10^{-3}	10.09	0.28	N.D.	N.D.	N.D.
F577E	20.53 ± 5.96	1.13 ± 0.07	55×10^{-3}	16.34	0.56	N.D.	23	N.D.
F577I	94.76 ± 27.26	0.58 ± 0.05	6.1×10^{-3}	83.2	0.8	95	48	76
F577K	112.3 ± 11.80	1.27 ± 0.04	11.3×10^{-3}	33.41	1.32	N.D.	N.D.	109
F577R	235.27 ± 50.06	0.77 ± 0.06	3.3×10^{-3}	49.21	1.38	N.D.	N.D.	50
F577W	25.4 ± 11.68	0.55 ± 0.05	21.7×10^{-3}	21.8	0.5	11	2	45
F577Y	8.78 ± 2.46	1.56 ± 0.08	177×10^{-3}	9.57	0.13	9	3	5

**Figure 3** Structures of three herbicides used in this study

(A) Londax, a sulphonylurea; (B) Cadre, an imidazolinone; (C) TP, a triazolopyrimidine.

around the aromatic amino acid residues, including the herbicide-binding site, appeared to have changed little in the mAHAS enzymes.

Taken together, the results suggest that the binding sites for the three classes of herbicides overlap partially, and that residue Phe-205 is located at the binding site common to the three herbicides.

Further, the binding site probably overlaps partially with the active site.

Phe-577 mutants

The Phe-577 mutants in which an uncharged amino acid was introduced, such as F577I, F577W and F577Y, were similar to wild-type AHAS with respect to the kinetic parameters for substrate and cofactors, and K_i^{app} values for the herbicides (Table 1). Although the mutants containing charged amino acids, such as F577D, F577E, F577K and F577R, were similar to wAHAS with regard to maximum enzymic activity, their catalytic efficiencies (V_{max}/K_m) were reduced substantially by a 4–63-fold (Table 1). The values of K_m and K_c for F577K and F577R, but not those of F577D and F577E, were markedly different from those of wAHAS (Table 1). The CD spectra of Phe-577 mutants in the far-UV spectral region were almost identical with that of the wild type (Figure 6 and results not shown). The CD spectra of F577D and F577R in the near-UV region overlapped completely with that of wAHAS (Figure 6B). However, the CD spectrum peak of F577E in the near-UV region was shifted from 265 to 276 nm. The inhibition of the Phe-577 mutants by three classes of herbicides showed differing cross-resistance profiles. F577D was strongly resistant to all three herbicides, while F577E showed strong cross-resistance to Londax and TP, and F577K and F577R were insensitive to Londax and Cadre (Table 1, Figures 4D and 4E). The results imply that Phe-577 is also located at the common binding site for the three herbicides.

Val-570 mutants

Although the V570N mutant of tobacco AHAS was expressed and purified as a soluble protein, it showed no detectable activity under various assay conditions, including much higher concentrations of substrate and cofactors and a longer incubation time. To understand the inactivation mechanism, the binding of the cofactor FAD to V570N mAHAS was determined by spectral measurements. Although the absorption spectrum of FAD bound to wAHAS was not well resolved, two peaks at around 370–390

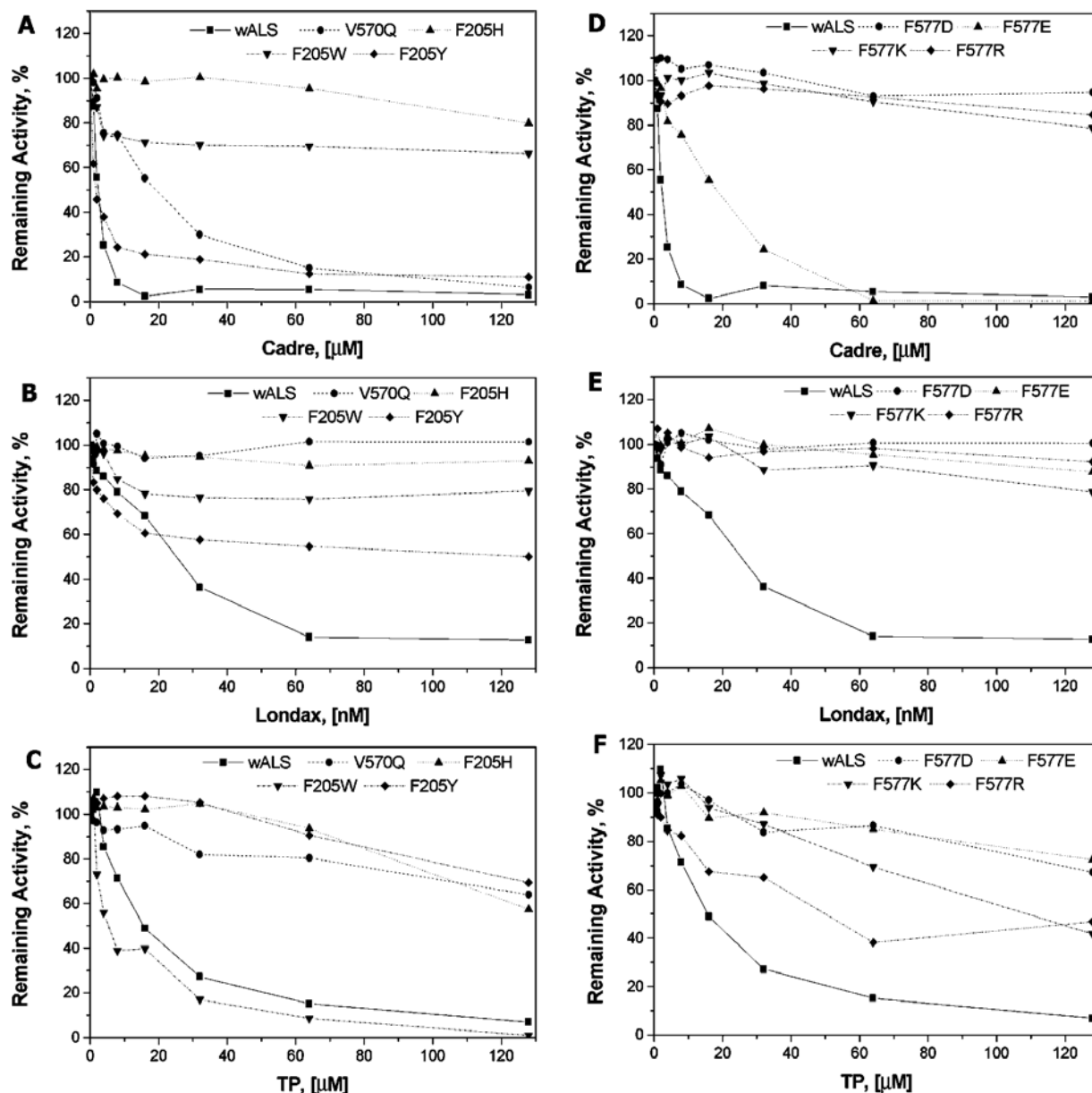


Figure 4 Inhibition of tobacco AHAS by three classes of herbicides: the imidazolinone Cadre (A, D), the sulphonylurea Londax (B, E) and the triazolopyrimidine TP (C, F)

wALS = wAHAS.

and 430–470 nm were evident (Figure 7), as reported previously [21]. In contrast, the spectrum of V570N showed no peak in the region 350–500 nm, superimposed on a background that rose progressively at a shorter wavelength (Figure 7). The fluorescence emission spectrum of FAD bound to V570N showed no peak around 530 nm on excitation at 370 nm, which is the emission peak of FAD bound to wAHAS (Figure 7, inset). Both the absorption and fluorescence spectra of V570N indicated that the mutant does not bind the cofactor FAD. The CD spectrum of V570N in the far-UV spectral region nearly overlapped with that of the wild type, but in the near-UV spectral region it showed a shift of the peak from 265 to 276 nm (Figure 8). The inactivation of AHAS by the mutation of Val-570 to Asn probably occurred due to loss of binding affinity for FAD. Val-570 is probably involved

in the binding of FAD, or a change in tertiary structure due to its mutation to Asn may interfere with the binding of FAD.

In contrast with V570N, the mutant V570Q remained active. The K_m value of V570Q was 129.2 mM, which is approx. 18-fold higher than that of wAHAS (Table 1). The K_c values of this mutant for FAD and TPP were almost 6- and 9-fold higher respectively than those of wAHAS. The V570Q mutant showed marked resistance to two classes of herbicide, Londax and TP (Table 1, Figures 4A–C). The CD spectra of this mutant overlapped almost completely with those of the wild type in both the far-UV and near-UV spectral regions (Figure 8), indicating that neither the secondary nor the tertiary structure was changed by the mutation.

The conservative substitution of Val-570 by Ile resulted in active mutant that displayed moderate changes in sensitivity to the three

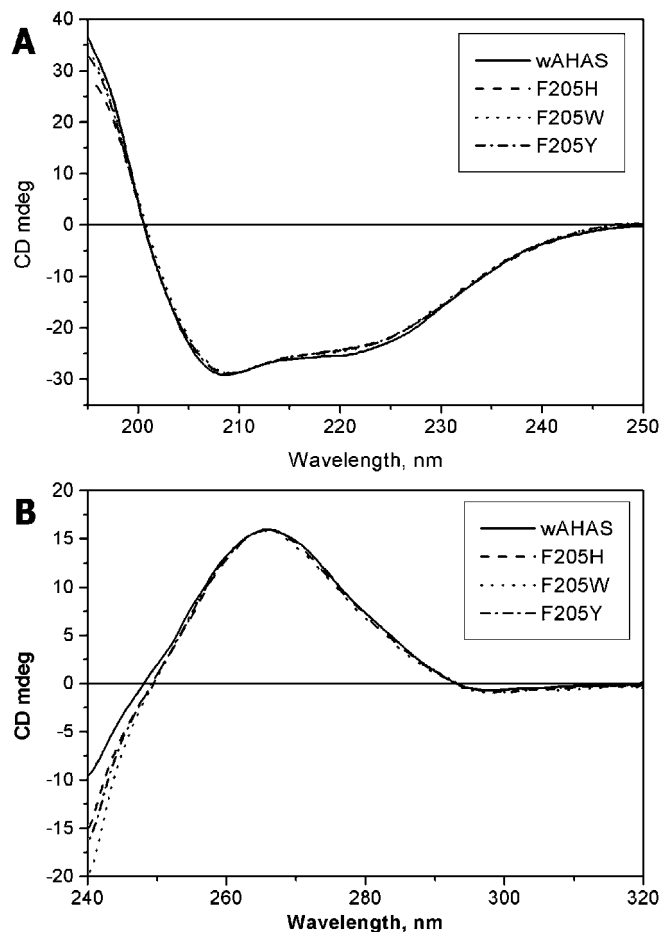


Figure 5 CD spectra of wAHAS and Phe-205 mutants

Each protein was present at a concentration of 0.25 mg/ml in 10 mM potassium phosphate buffer (pH 7.5). (A) Far-UV CD spectra; (B) near-UV CD spectra.

tested herbicides. However, its K_m value was increased and its V_{max} value was decreased compared with wAHAS. The overall catalytic efficiency of the conservative mutant was 30-fold lower than that of the wild-type enzyme.

Overall, the results following mutation of Val-570 suggest that this residue is located at the herbicide-binding site, and that the site may overlap with the active site.

DISCUSSION

Since the first two plant AHAS genes were isolated from *Arabidopsis thaliana* and *Nicotina tabacum* using the yeast gene *ilv2* [9], a number of plant AHAS genes have been cloned and characterized [9–13]. Subsequently it became possible to express the plant genes at a high level using a suitable expression system and to purify the enzyme to homogeneity [14,15].

More recently, crystallization and preliminary X-ray diffraction analysis of the catalytic subunit of *Saccharomyces cerevisiae* AHAS have been reported [26,27]. A homology model of tobacco AHAS based on the yeast AHAS was constructed using the Swiss-Model server [28,29]. The homology model of tobacco AHAS was proved to be reliable on the basis of modelling the structure through the Ramachandran plot (results not shown), its RMS Z-score and the pairwise RMSD value of 0.86 Å when the

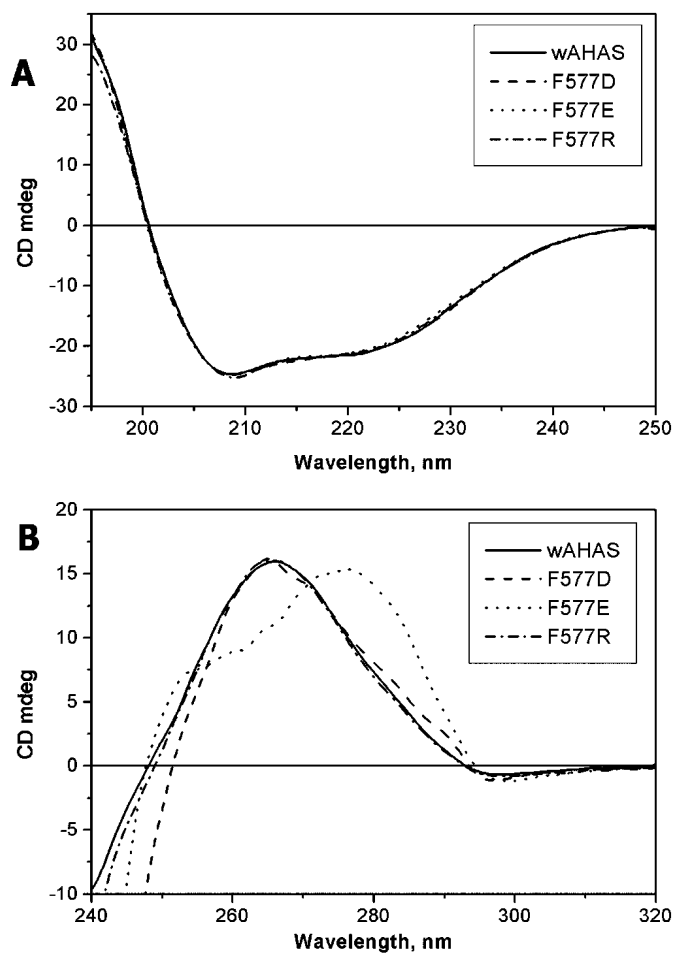


Figure 6 CD spectra of wAHAS and Phe-577 mutants

Each protein was present at a concentration of 0.25 mg/ml in 10 mM potassium phosphate buffer (pH 7.5). (A) Far-UV CD spectra; (B) near-UV CD spectra.

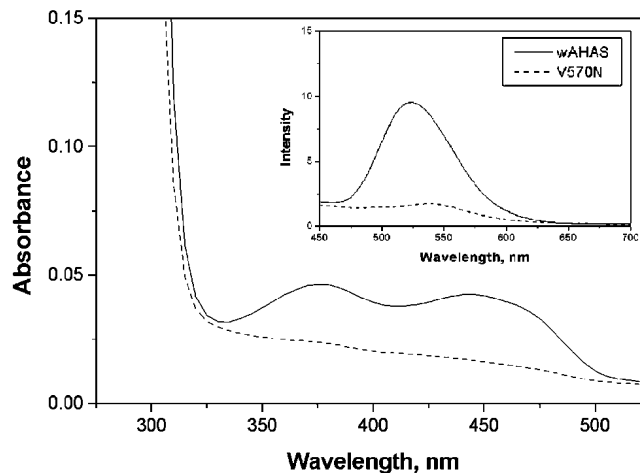


Figure 7 Absorption spectra of wAHAS (solid line) and the V570N mutant (broken line)

The concentration of each enzyme was 1.2 mg of protein/ml in 50 mM Tris/HCl buffer (pH 7.5). The inset shows the fluorescence spectra of wAHAS and the V570N mutant under the same conditions.

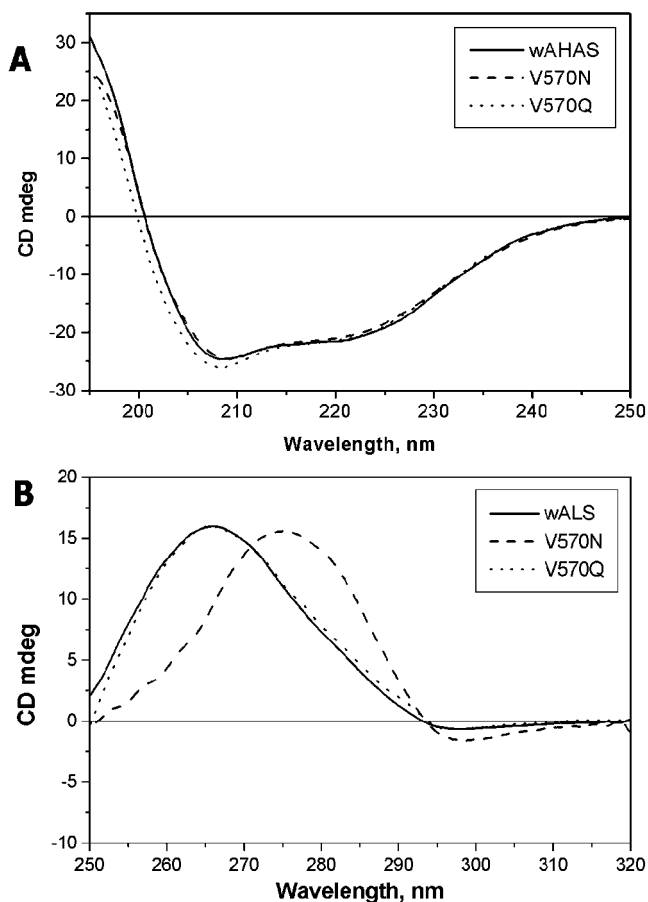


Figure 8 CD spectra of wAHAS and Val-570 mutants

Each protein was present at a concentration of 0.25 mg/ml in 10 mM potassium phosphate buffer (pH 7.5). (A) Far-UV CD spectra; (B) near-UV CD spectra.

tobacco AHAS model was superimposed on the yeast AHAS structure (results not shown).

Using the constructed homology model, seven residues of monomer A and 11 residues of monomer B were identified to be neighbouring residues within 5 Å of a bound sulphonylurea, chlorimuron ethyl (Figure 2; other six residues not shown). Among these, residues Phe-205, Val-570 and Phe-577 were found to be well conserved, as revealed by multiple sequence alignment of AHASs from 33 species (Figure 1). Accordingly, the roles of Phe-205, Val-570 and Phe-577 were investigated by site-directed mutagenesis. All mutants of tobacco AHAS were successfully generated and expressed as soluble forms, and purified to homogeneity (results not shown). Each of the mutant enzymes was characterized with respect to its kinetic properties, including V_{\max} , K_m , V_{\max}/K_m , K_c values for FAD and TPP, and K_i^{app} values for the three herbicides Londax, Cadre and TP (Table 1 and Figure 4).

The mutations of F205A, F205H, F205W and F205Y resulted in greatly decreased catalytic efficiency (Table 1). On the other hand, the Phe-205 mutants were cross-resistant to two or three of the herbicides Cadre, Londax and TP without changes in either the secondary or tertiary structure (Table 1, Figures 4 and 5 and results not shown). According to the homology model, the binding sites for FAD and herbicides are located close together, and residue Phe-205 is found to be the neighbouring residue of both FAD and herbicide (Figure 2). In addition, it was reported previously

that the active site and herbicide-binding site of yeast AHAS partially overlap [41]. Therefore Phe-205 is probably located at the common herbicide-binding site which may partially overlap with the active site of AHAS.

The mutant enzymes in which Phe-577 was substituted by a non-charged amino acid showed similar kinetic properties for substrate and cofactors FAD and TPP, and K_i^{app} values for the herbicides Cadre, Londax and TP, compared with wAHAS (Table 1). Though the Phe-577 mutants containing charged amino acids (F577D, F577E, F577K and F577R) showed similar V_{\max} values to the wild type, their catalytic efficiencies were decreased substantially by 4–63-fold. However, they were strongly cross-resistant to two or three classes of herbicides represented by Cadre, Londax and TP (Table 1, Figure 4). Phe-577 is found at an entrance of the herbicide-binding site, and the surroundings of Phe-577 appear to be a hydrophobic region contributed by hydrophobic residues such as Trp-573 and Tyr-578 in the tobacco AHAS homology model (Figure 2). Thus we propose that the hydrophobic features of the herbicides approach the binding site by hydrophobic force. However, the herbicide cannot approach in this way in mutants where a charged amino acid is present at residue 577, because a hydrophobic region is not formed. AHAS mutants in which residue 577 is a negatively charged amino acid could be used to construct herbicide-resistant transgenic plants, since some of the mutations do not reduce catalytic efficiency significantly, but confer strong herbicide-resistance.

The replacement of Val-570 by Asn, which has an uncharged polar side chain, caused the enzyme to be totally inactive under various assay conditions (Table 1). To understand the mechanism of inactivation, the spectroscopic properties of V570N were compared with those of wAHAS. The results showed that mutant V570N did not give any absorption or fluorescence emission peaks corresponding to FAD bound to mutant AHAS, in contrast with wAHAS (Figure 7) [21]. Thus V570N had lost its affinity for FAD, and consequently the mutant was inactive. Although the secondary structure of V570N was similar to that of the wild-type, the tertiary structure was different (Figure 8). In the tobacco AHAS homology model, residue Val-570 is not very close to bound FAD (Figure 2). Thus it is proposed that the V570N mutant loses its binding affinity for FAD due to a change in the local tertiary structure.

The mutant V570Q is active, but shows a strong resistance to two classes of herbicides, represented by Londax and TP (Table 1, Figure 4). The CD spectrum of this mutant overlapped almost completely with that of the wild type in both the far-UV and near-UV spectral regions (Figure 8), indicating that structural changes did not occur as a result of the mutation. The conservative mutant V570I showed moderate resistance to the three herbicides; however, its catalytic efficiency was reduced by 30-fold. Thus the results imply that Val-570 is probably located at an herbicide-binding site of AHAS that may partly overlap with the active site.

Almost all mutants of Phe-205, Phe-577 and Val-570 showed strong cross-resistance to the three classes of herbicides investigated. Thus these three residues are probably located at or near a common binding site for the three classes of herbicides. Furthermore, Phe-205 and Val-570 are probably located at a herbicide-binding site that overlaps partly with the active site. According to the X-ray structure of yeast AHAS, the sulphonylurea-binding site is located at the dimer interface, and is in the vicinity of the active site and the flavin ring of FAD [41]. The results obtained in the present study imply that the constructed homology model of tobacco AHAS is quite reliable, and are also consistent with the model of *Arabidopsis thaliana* AHAS based on the X-ray

structure of TPP-containing pyruvate oxidase [14]. Our results also indicate that selected mutants in which Phe-577 was altered could be used to construct herbicide-resistant crops.

We thank Dr Dae-Whang Kim (Korea Research Institute of Chemical Technology, Korea) for Londa and Cadre, and Dr Sung-Keon Namgoong (Seoul Women's University, Korea) for TP. This work was supported by the Korea Research Foundation, grant KRF-2002-070-C0064.

REFERENCES

- Duggleby, R. G. and Pang, S. S. (2000) Acetohydroxyacid Synthase. *J. Biochem. Mol. Biol.* **33**, 1–36
- Gollop, N., Chipman, D. M. and Barak, Z. (1983) Kinetics and mechanism of acetohydroxy acid synthase isozyme III from *Escherichia coli*. *Biochim. Biophys. Acta* **748**, 34–39
- Schloss, J. V., Dyk, K. E. V., Vasta, J. F. and Kutny, B. M. (1985) Purification and properties of *Salmonella typhimurium* acetolactate synthase isozyme II from *Escherichia coli* HB101/pDU. *Biochemistry* **24**, 4952–4959
- Grimminger, H. and Umbarger, H. E. (1979) Acetohydroxyacid synthase I of *Escherichia coli*: purification and properties. *J. Bacteriol.* **137**, 846–853
- Ryan, E. D. and Kohlhow, G. B. (1974) Subcellular localization of isoleucine-valine biosynthetic enzymes in yeast. *J. Bacteriol.* **120**, 631–637
- Barak, Z., Chipman, D. M. and Gollop, N. (1987) Physiological implications of the specificity of acetohydroxyacid synthase isozymes of enteric bacteria. *J. Bacteriol.* **169**, 3750–3756
- Eoyang, L. and Silverman, P. M. (1988) Branched-chain amino acids. *Methods Enzymol.* **166**, 435–445
- Hill, C. M. and Duggleby, R. G. (1998) Mutagenesis of *Escherichia coli* acetohydroxyacid synthase isoenzyme II and characterization of three herbicide-insensitive forms. *Biochem. J.* **335**, 653–661
- Mazur, B. J., Chui, C.-F. and Smith, J. K. (1987) Isolation and characterization of plant genes coding for acetolactate synthase, the target enzyme for two classes of herbicides. *Plant Physiol.* **75**, 1110–1117
- Hattori, J., Rutledge, R. G., Miki, B. L. and Baum, B. R. (1992) Multiple resistance to sulfonyleureas and imidazolinones conferred by an acetohydroxyacid synthase gene with separate mutations for selective resistance. *Mol. Gen. Genet.* **232**, 167–173
- Gruha, J. W., Hudspeth, R. L., Hobbs, S. L. and Anderson, D. M. (1995) Organization, inheritance and expression of acetohydroxyacid synthase genes in the cotton allotetraploid *Gossypium hirsutum*. *Plant Mol. Biol.* **28**, 837–846
- Fang, G. Y., Gross, P. R., Chen, C. H. and Lillis, M. (1992) Sequence of two acetohydroxyacid synthase genes from *Zea mays*. *Plant Mol. Biol.* **12**, 1185–1187
- Bernasconi, P., Woodworth, A. R., Rosen, B. A., Subramanian, M. V. and Siehl, D. L. (1995) A naturally occurring point mutation confers broad range tolerance to herbicides that target acetolactate synthase. *J. Biol. Chem.* **270**, 17381–17385
- Ott, K.-H., Kwagh, J.-G., Stockton, G. W., Sidrov, V. and Kekefuva, G. (1996) Rational molecular design and genetic engineering of herbicide resistance crops by structure modeling and site-directed mutagenesis of acetohydroxyacid synthase. *J. Mol. Biol.* **263**, 359–367
- Chang, S.-I., Kang, M.-K., Choi, J.-D. and Namgoong, S. K. (1997) Soluble expression in *Escherichia coli*, and purification and characterization of wild-type recombinant tobacco acetolactate synthase. *Biochem. Biophys. Res. Commun.* **234**, 549–553
- LaRossa, R. A. and Schloss, J. V. (1984) The sulfonyleurea herbicide sulfonureton methyl is an extremely potent and selective inhibitor of acetolactate synthase in *Salmonella typhimurium*. *J. Biol. Chem.* **259**, 8753–8757
- Ray, T. B. (1984) Site of action of chlorsulfuron: inhibition of valine and isoleucine biosynthesis of plants. *Plant Physiol.* **75**, 827–831
- Shaner, D. L., Anderson, P. C. and Stidham, M. A. (1984) Imidazolinones: potent inhibitors of acetohydroxyacid synthase. *Plant Physiol.* **76**, 545–546
- Gerwick, B. C., Subramanian, M. V., Loney-Gallant, V. and Chander, D. P. (1990) Mechanism of action of the 1,2,4-triazolo[1,5-a]pyrimidine. *Pestic. Sci.* **29**, 357–364
- Namgoong, S. K., Lee, H. J., Kim, Y. S., Shin, J.-H., Che, J.-K., Jang, D. Y., Kim, G. S., Yoo, J. W., Kang, M.-K., Kil, M.-W. et al. (1999) Synthesis of the quinoline-linked triazolopyrimidine analogues and their interaction with the recombinant tobacco acetolactate synthase. *Biochem. Biophys. Res. Commun.* **258**, 797–801
- Chong, C.-K., Shin, H.-J., Chang, S.-I. and Choi, J.-D. (1999) Role of tryptophanyl residues in tobacco acetolactate synthase. *Biochem. Biophys. Res. Commun.* **259**, 136–140
- Chong, C.-K. and Choi, J.-D. (2000) Amino acid residues conferring herbicide tolerance in tobacco acetolactate synthase. *Biochem. Biophys. Res. Commun.* **279**, 462–467
- Oh, K.-J., Park, E.-J., Yoon, M.-Y., Han, J.-R. and Choi, J.-D. (2001) Roles of histidine residues in tobacco acetolactate synthase. *Biochem. Biophys. Res. Commun.* **282**, 1237–1243
- Yoon, T.-Y., Chung, S.-M., Chang, S.-I., Yoon, M.-Y., Hahn, T.-R. and Choi, J.-D. (2002) Roles of lysine 219 and 255 residues in tobacco acetolactate synthase. *Biochem. Biophys. Res. Commun.* **293**, 433–439
- Le, D. T., Yoon, M.-Y., Kim, Y.-T. and Choi, J.-D. (2003) Roles of conserved methionine residues in tobacco acetolactate synthase. *Biochem. Biophys. Res. Commun.* **306**, 1075–1082
- Pang, S.-S., Guddat, L.-W. and Duggleby, R.-G. (2001) Crystallization of the catalytic subunit of *Saccharomyces cerevisiae* acetohydroxyacid synthase. *Acta Crystallogr.* **D57**, 1321–1323
- Pang, S.-S., Duggleby, R.-G. and Guddat, L.-W. (2002) Crystal structure of yeast acetohydroxyacid synthase: A target for herbicidal inhibitors. *J. Mol. Biol.* **317**, 249–262
- Schwede, T., Kopp, J., Guex, N. and Peitsch, M.-C. (2003) SWISS-MODEL: an automated protein homology-modeling server. *Nucleic Acids Res.* **31**, 3381–3385
- Guex, N. and Peitsch, M. C. (1997) SWISS-MODEL and the Swiss-PdbViewer: An environment for comparative protein modelling. *Electrophoresis* **18**, 2714–2723
- Hall, T. A. (1999) BioEdit: a user-friendly biological sequence alignment editor and analysis program for Windows 95/98/NT. *Nucleic Acids Symp. Ser.* **41**, 95–99
- Thompson, J. D., Higgins, D. G. and Gibson, T. J. (1994) CLUSTALW: improving the sensitivity of progressive multiple sequence alignment through sequence weighting, position-specific gap penalties and weight matrix choice. *Nucleic Acids Res.* **22**, 4673–4680
- Sarkar, G. and Sommer, S. S. (1990) 'Megaprimer' method of site-directed mutagenesis. *Biotechniques* **2**, 404–407
- Sambrook, J., Fritsch, E. F. and Maniatis, T. (1989) *Molecular Cloning: A Laboratory Manual*, 2nd edn., Cold Spring Harbor Laboratory Press, Cold Spring Harbor, NY
- Saiki, R. K., Gelfand, D. H., Stoffel, S., Scharf, S. J., Higuchi, R., Horn, G. T., Mullis, K. B. and Erlich, H. A. (1988) Primer-directed enzymatic amplification of DNA with a thermostable DNA polymerase. *Science* **239**, 487–491
- Laemmli, U. K. (1970) Cleavage of structural proteins during the assembly of the head of bacteriophage T4. *Nature (London)* **227**, 680–685
- Bradford, M. M. (1976) A rapid and sensitive method for the quantification of microgram quantities of protein utilizing the principle of protein-dye binding. *Anal. Biochem.* **72**, 248–254
- Westerfeld, W. W. (1945) A colorimetric determination of blood acetoin. *J. Biol. Chem.* **161**, 495–502
- Smith, J. K., Schloss, J. V. and Mazur, B. J. (1989) Functional expression of plant acetolactate synthase genes in *Escherichia coli*. *Proc. Natl. Acad. Sci. U.S.A.* **86**, 4179–4183
- Nelder, J. A. and Mead, R. (1965) A simple method for function minimization. *Comput. J.* **7**, 308–313
- Kelly, S.-M. and Price, N.-C. (1997) The application of circular dichroism to studies of protein folding and unfolding. *Biochim. Biophys. Acta* **1338**, 161–185
- Pang, S. S., Guddat, L. W. and Duggleby, R. G. (2003) Molecular basis of sulfonyleurea herbicide inhibition of acetohydroxy acid synthase. *J. Biol. Chem.* **278**, 7639–7644

Received 30 April 2004/4 June 2004; accepted 24 June 2004

Published as BJ Immediate Publication 24 June 2004, DOI 10.1042/BJ20040720